SSAA/SGAA General Assembly

Locarno, Palazzo Morettini, 15.– 16. 10., 2015

Why numerical simulations?

Oskar Steiner

Istituto Ricerche Solari Locarno (IRSOL), Locarno Monti, Switzerland

Kiepenheuer-Institut für Sonnenphysik, Freiburg i.Br., Germany

1. Understanding polarimetry with simulations

Spectral line (Stokes I) and corresponding Stokes V (schematic).

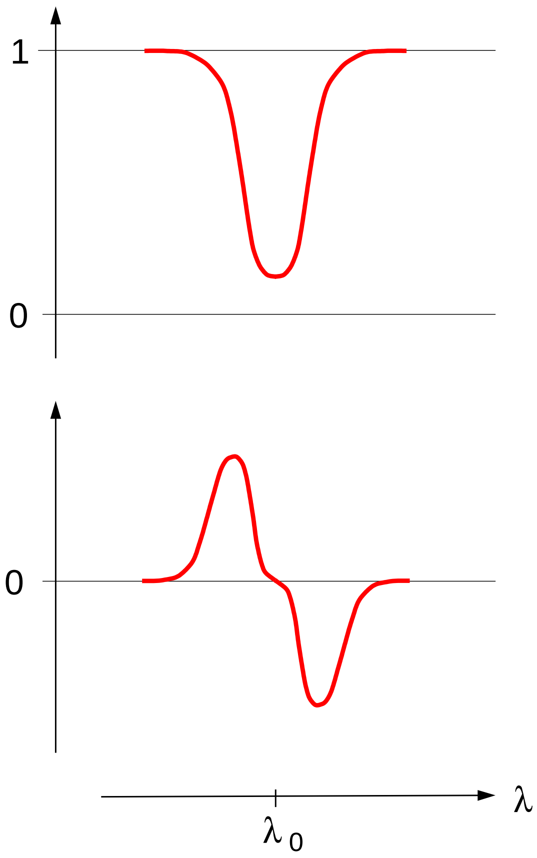

Due to the *Zeeman-effect*, left or right circularly polarized light emanates from the flanks of a magnetically sensitive spectral line. *Stokes* V is the difference between right and left circularly polarized light.

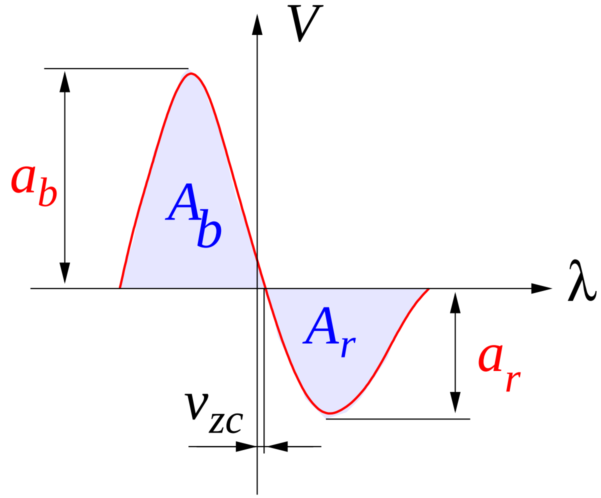

1. Understanding polarimetry with simulations (cont.): observation

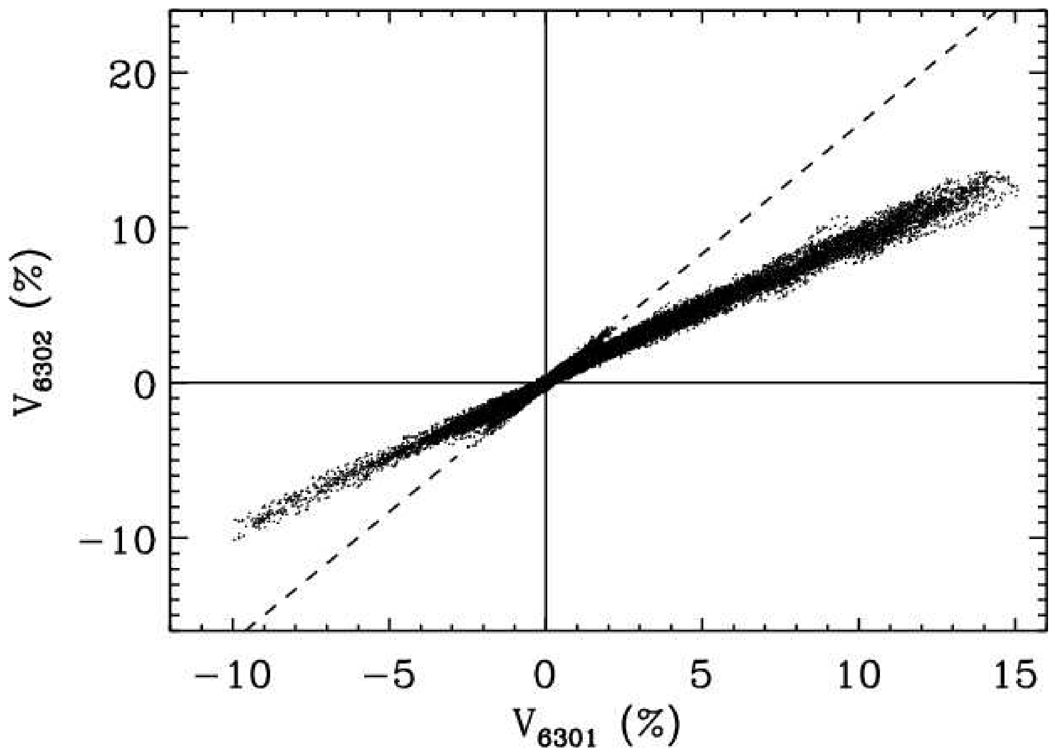

Weak field limit: $V \sim g(\partial I/\partial\lambda) \quad\Rightarrow$

$$\frac{V_{6302}^{\mathrm{peak}}}{V_{6301}^{\mathrm{peak}}} = \frac{g_{6302}}{g_{6301}}\,\frac{(\partial I/\partial\lambda)_{6302}^{\max}}{(\partial I/\partial\lambda)_{6301}^{\max}}$$

$$= \frac{2.5}{1.667}\,\frac{(\partial I/\partial\lambda)_{6302}^{\max}}{(\partial I/\partial\lambda)_{6301}^{\max}}$$

$$\approx 1.5\cdot 1.1 \approx 1.66$$

$\Rightarrow$ Section at 1%

Bivariate scatter of the Stokes-V amplitudes of the 6302.5 Å line vs. the 6301.5 Å line as *observed with Hinode/SOT/SP*. The dashed line with slope s=1.66 represents the regression relation expected for weak fields. We identify *two populations of points*. From *Stenflo (2010) A&A 517 A37*.

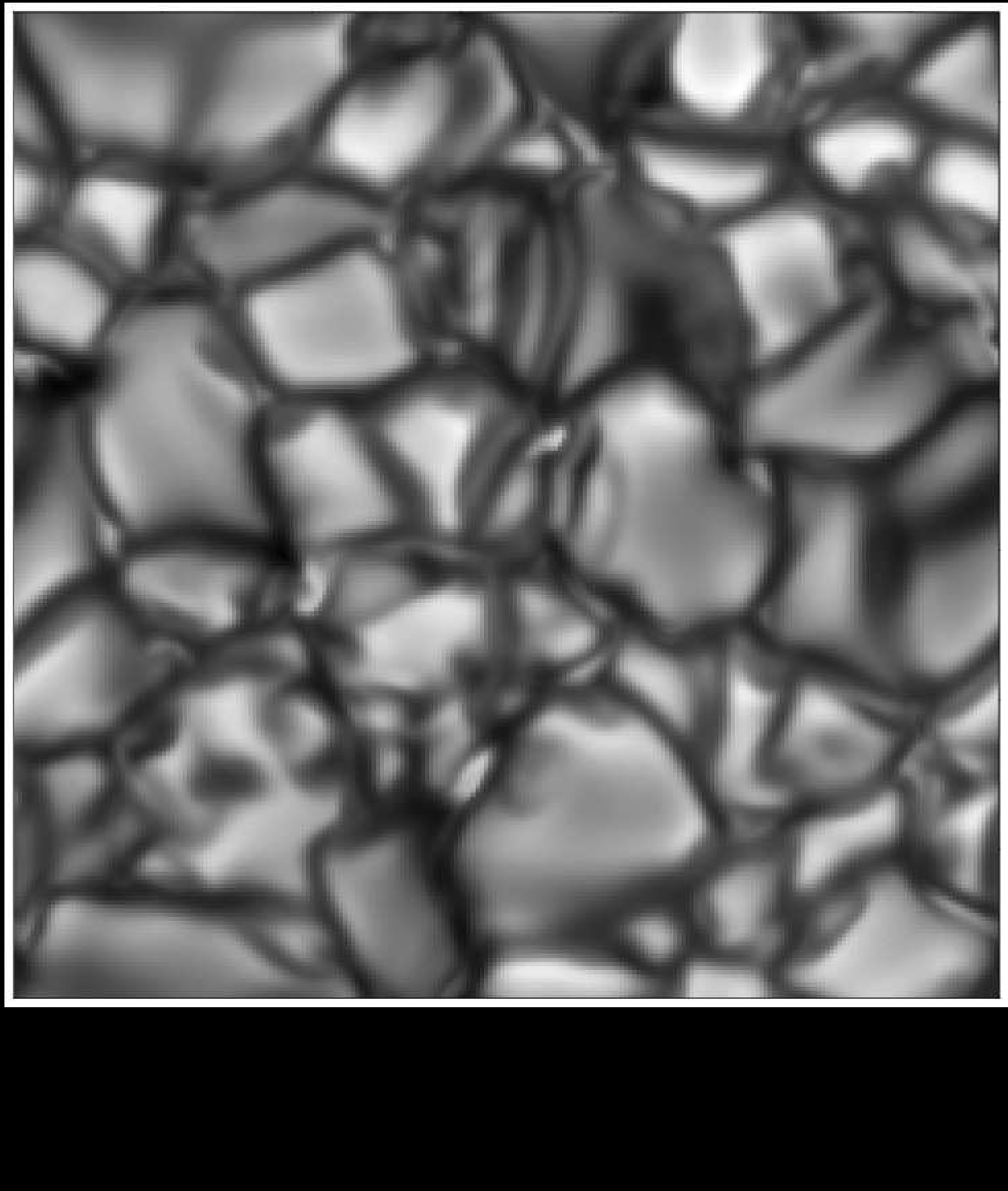

1. Understanding polarimetry with simulations (cont.): simulation data

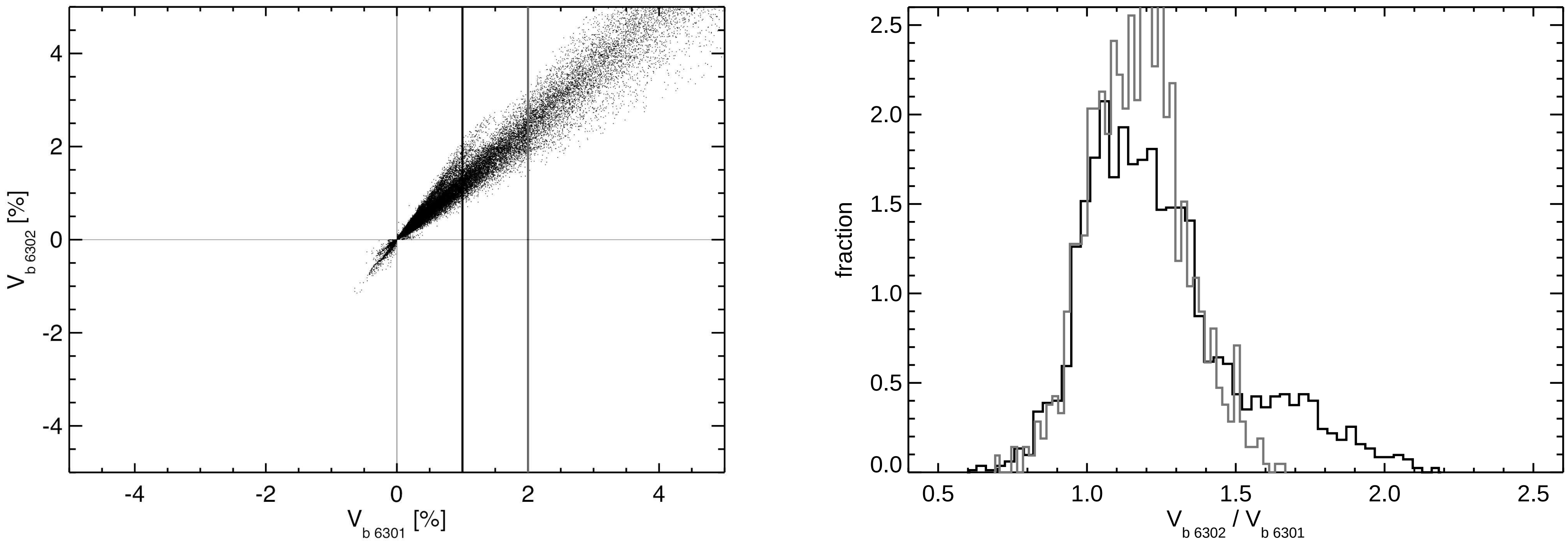

Scatter plot of Stokes-V amplitudes of two lines and histogram of the line ratio at two different amplitude levels from the simulation. From *Steiner & Rezaei (2012)*.

1. Understanding polarimetry with simulations (cont.): simulation data

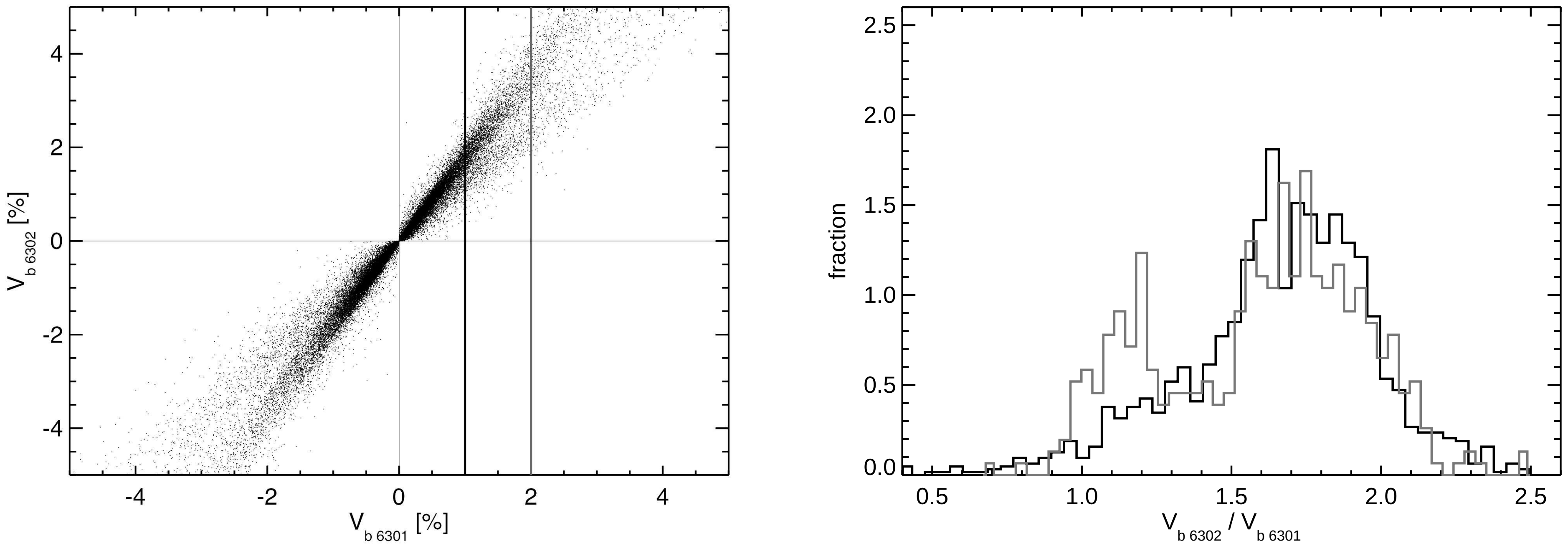

Left: Scatter plot of the Stokes-V amplitude of Fe I 630.250 nm vs. that of Fe I 630.151 nm of synthesized V profiles from MHD simulation h50. The scatter is from pixels at full spatial resolution. *Right:* Corresponding histogram of the points that fall within the range $0.8 \leq V_{630.15} \leq 1.0$ (black) and $1.8 \leq V_{630.15} \leq 2.0$ (gray).

From *Steiner & Rezaei (2012), Hinode 5 Proc.*

"It is nice to know that the computer understands the problem, but I would like to understand it too."

Attributed to E.P. Wigner

“It is nice to know that the computer understands the problem, but I would like to understand it too.”

Attributed to E.P. Wigner

“It is nice to know that our simulations reproduce the observations, but what can we learn from it?”

1. Understanding polarimetry with simulations (cont.)

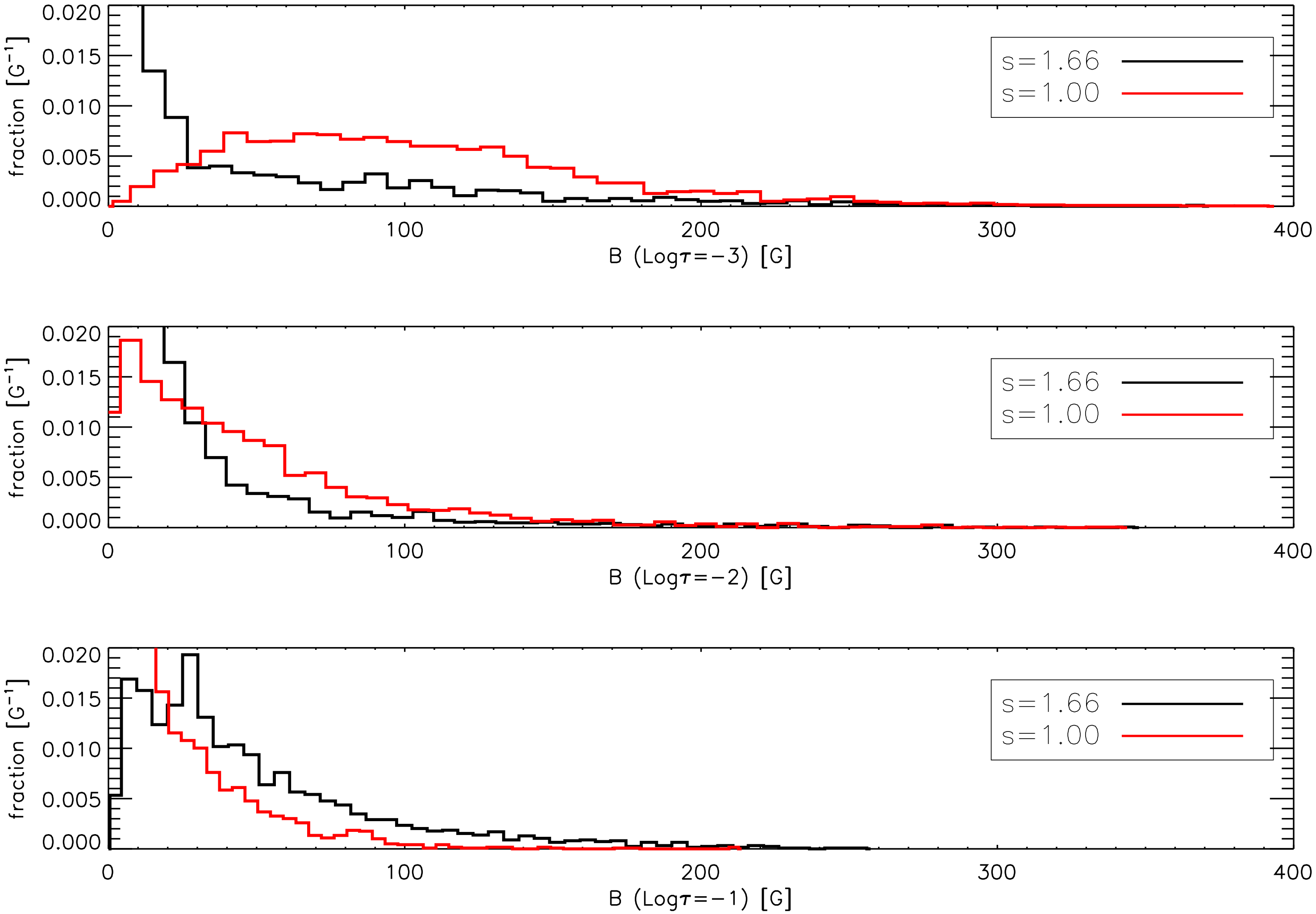

$\log\tau = -3$

$\log\tau = -2$

$\log\tau = -1$

Histogram of the *field strength* at different heights for the two populations of line-ratios from run v50 and for pixels with $1.0 \leq V_{\mathrm{b}\,6301} \leq 2.0$. $s = \langle V_{\mathrm{b}\,6302} / V_{\mathrm{b}\,6301} \rangle$. *Steiner & Rezaei (2012)*

2. Understanding polarimetry with simulations (cont.)

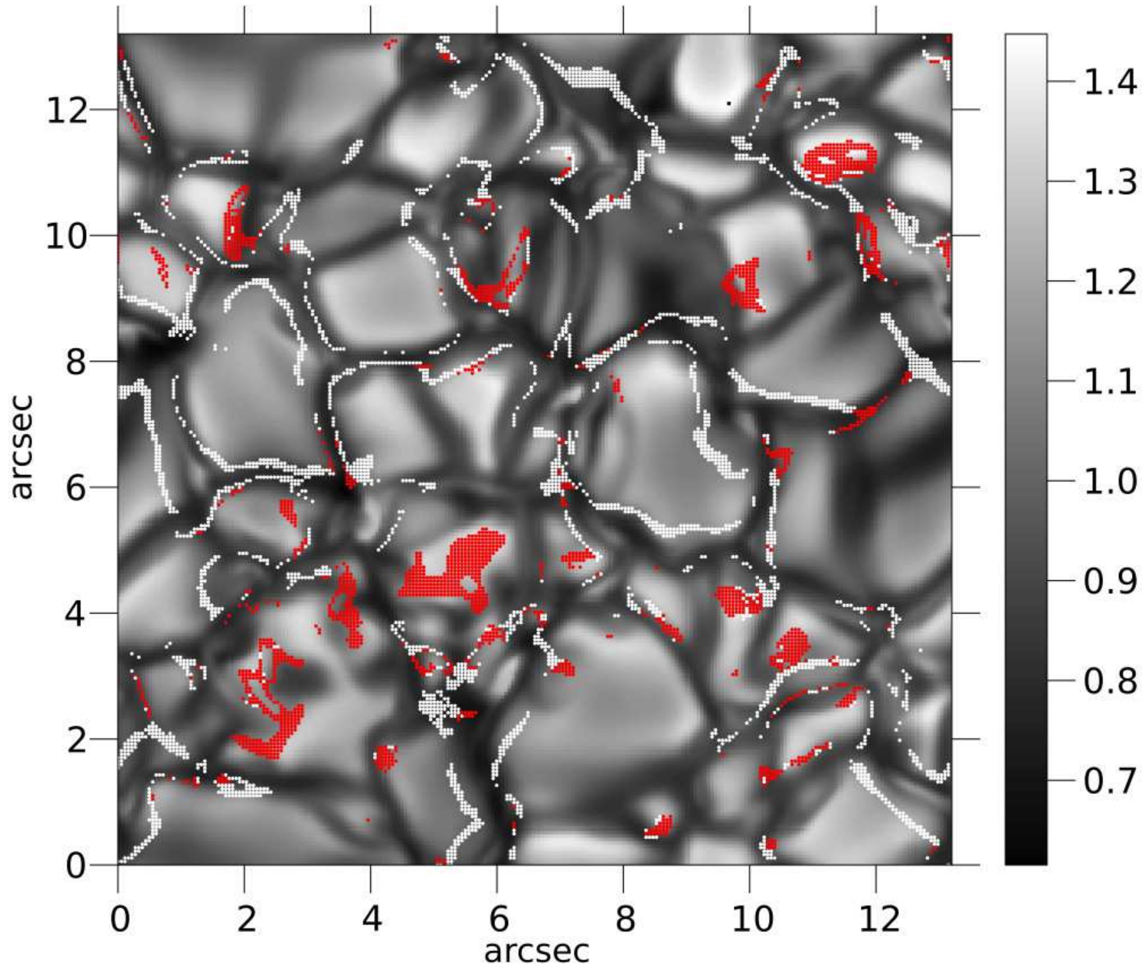

White: Pixels with polarization level $1.0 \leq V_{630.15} \leq 2.0$ belonging to the population with $V^{\rm b}_{630.25}/V^{\rm b}_{630.15} \leq 1.5$ (first, main population). *Red:* Pixels with polarization level $1.0 \leq V_{630.15} \leq 2.0$ belonging to the population with $V^{\rm b}_{630.25}/V^{\rm b}_{630.15} \geq 1.5$ (second, intrinsic weak field population). *Background:* Continuum intensity at 630 nm. From *Steiner & Rezaei (2012) Hinode 5 Proc.*

Conclusion: The two populations can be explained in terms of weak (hectogauss) magnetic fields. *Numerical simulations are indispensable for the correct interpretation.*

2. Numerical simulations at IRSOL

Solar granulation *observed* with the new 1.4 m GREGOR solar telescope. Broad-band filter at $\lambda = 4860$ Å.

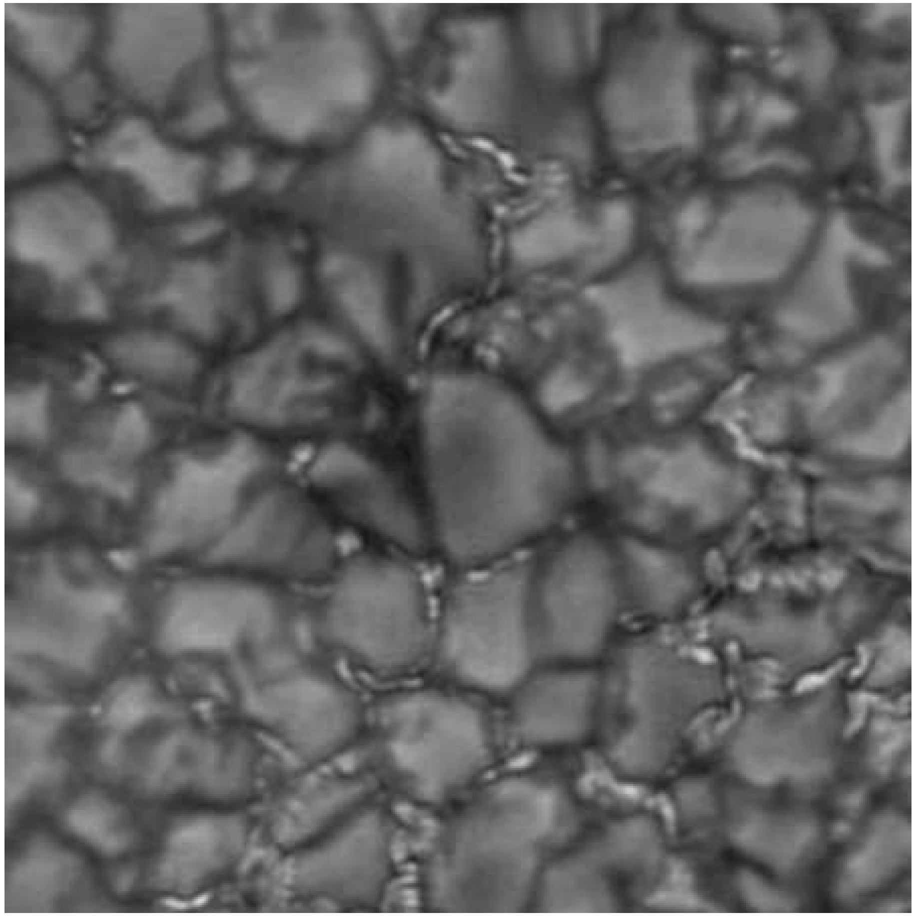

Solar granulation *simulated* with the CO^{5}BOLD radiation MHD code. Synthetic map of bolometric intensity.

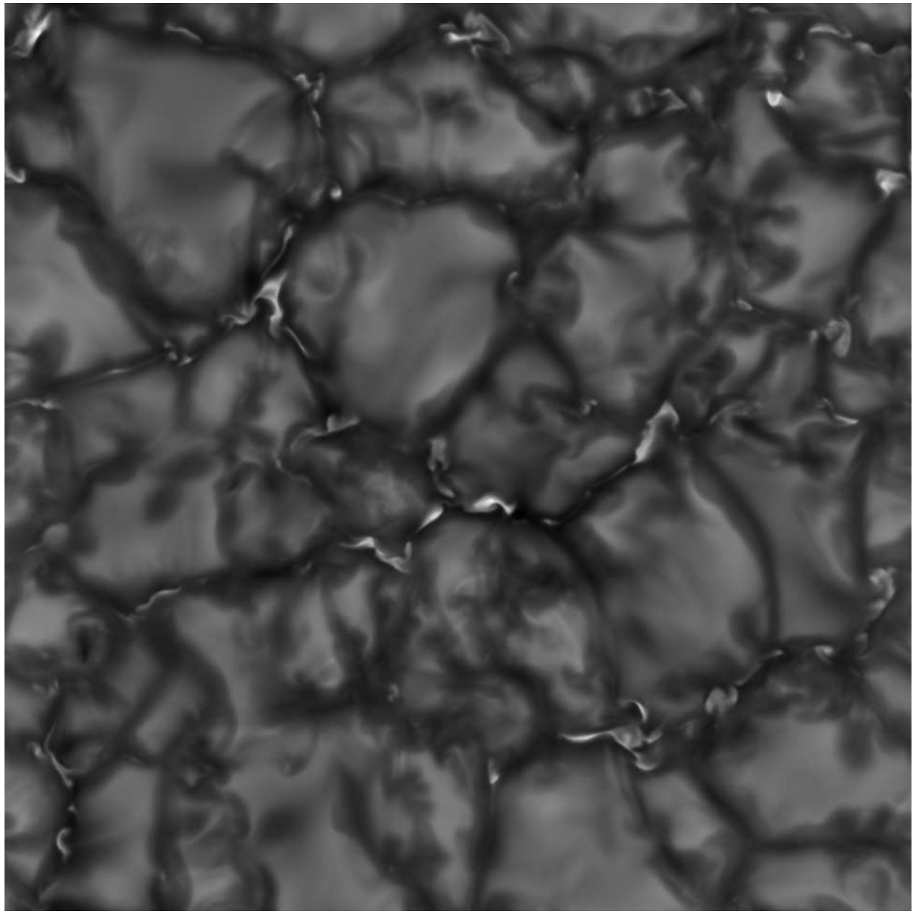

Numerical simulations at IRSOL (cont.)

Bolometric intensity maps (CO^{5}BOLD simulations, $\Delta x = \Delta y = \Delta z = 10$ km)

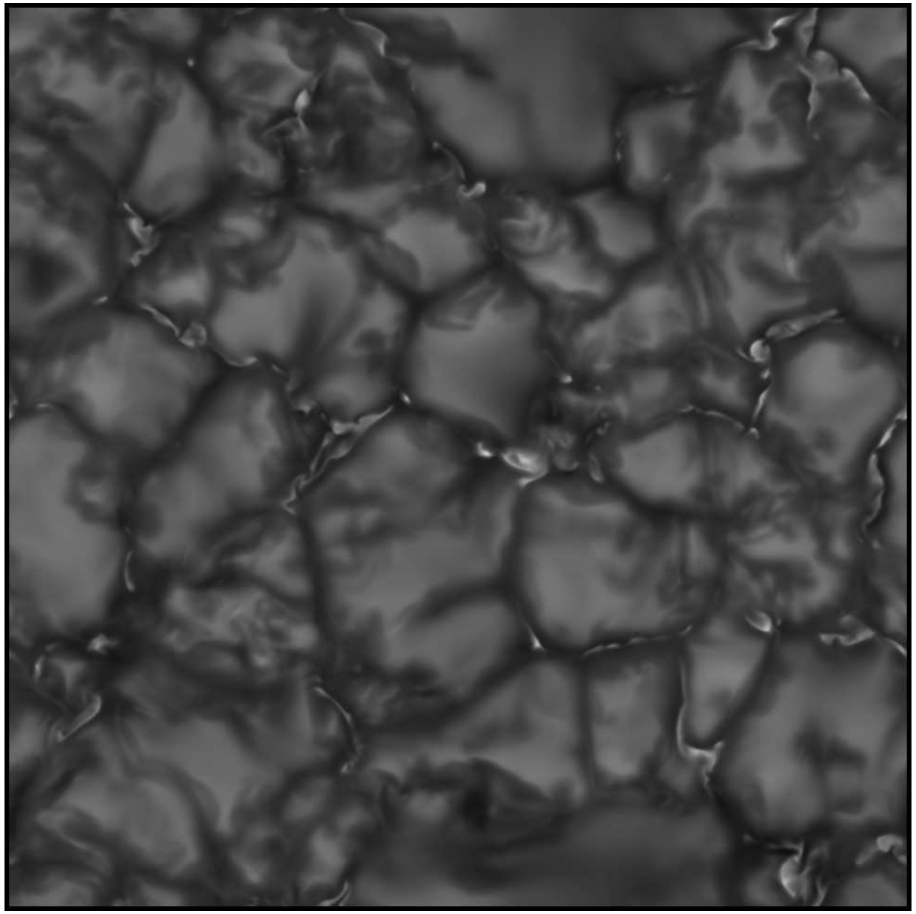

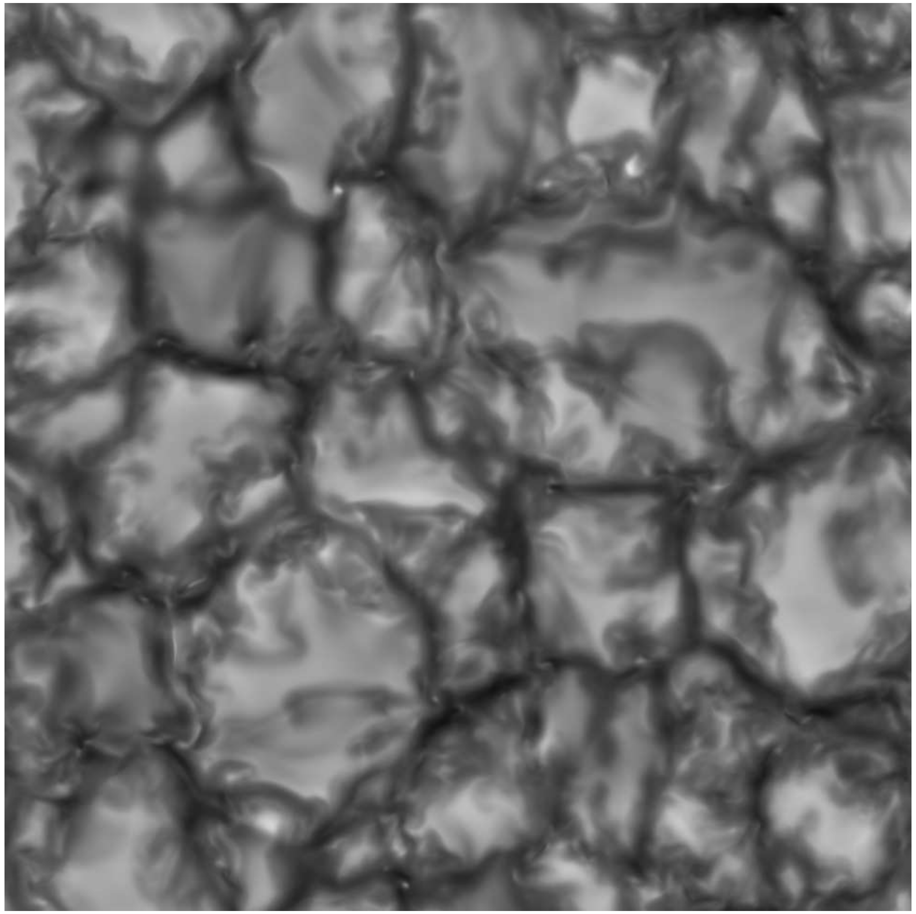

Computations: *Centro Svizzero di Calcolo Scientifico*

With magnetic fields:
magnetic bright points.

Without magnetic fields:
non-magnetic bright points

Courtesy,
F. Calvo.

Slices across a non-magnetic bright point (nMBP0868)

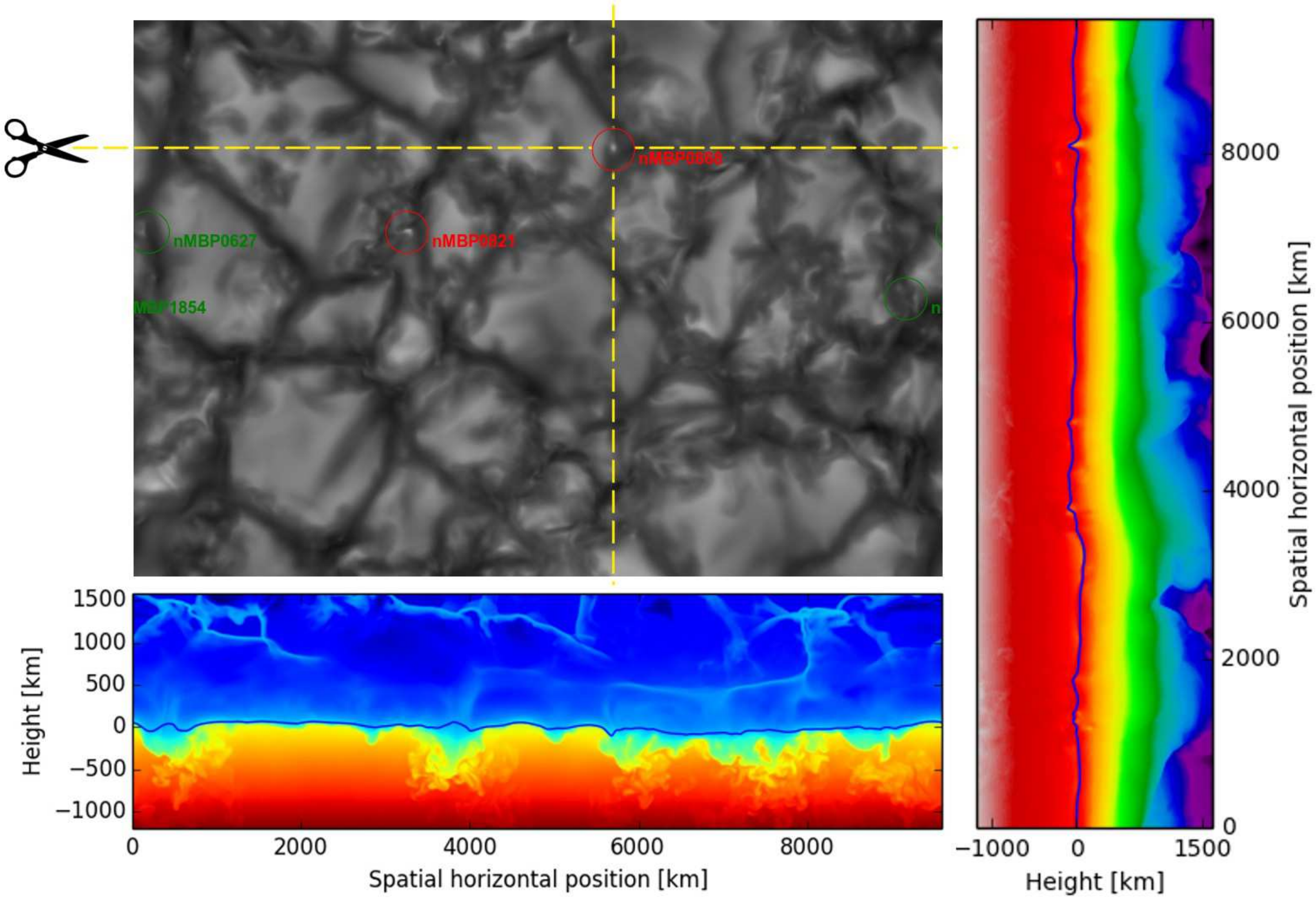

Courtesy, *F. Calvo IRSOL*.

Emergent intensity I (*top left*), temperature T (*bottom*), density $\log(\rho)$ (*right*)

Slices across a non-magnetic bright point (nMBP0868)

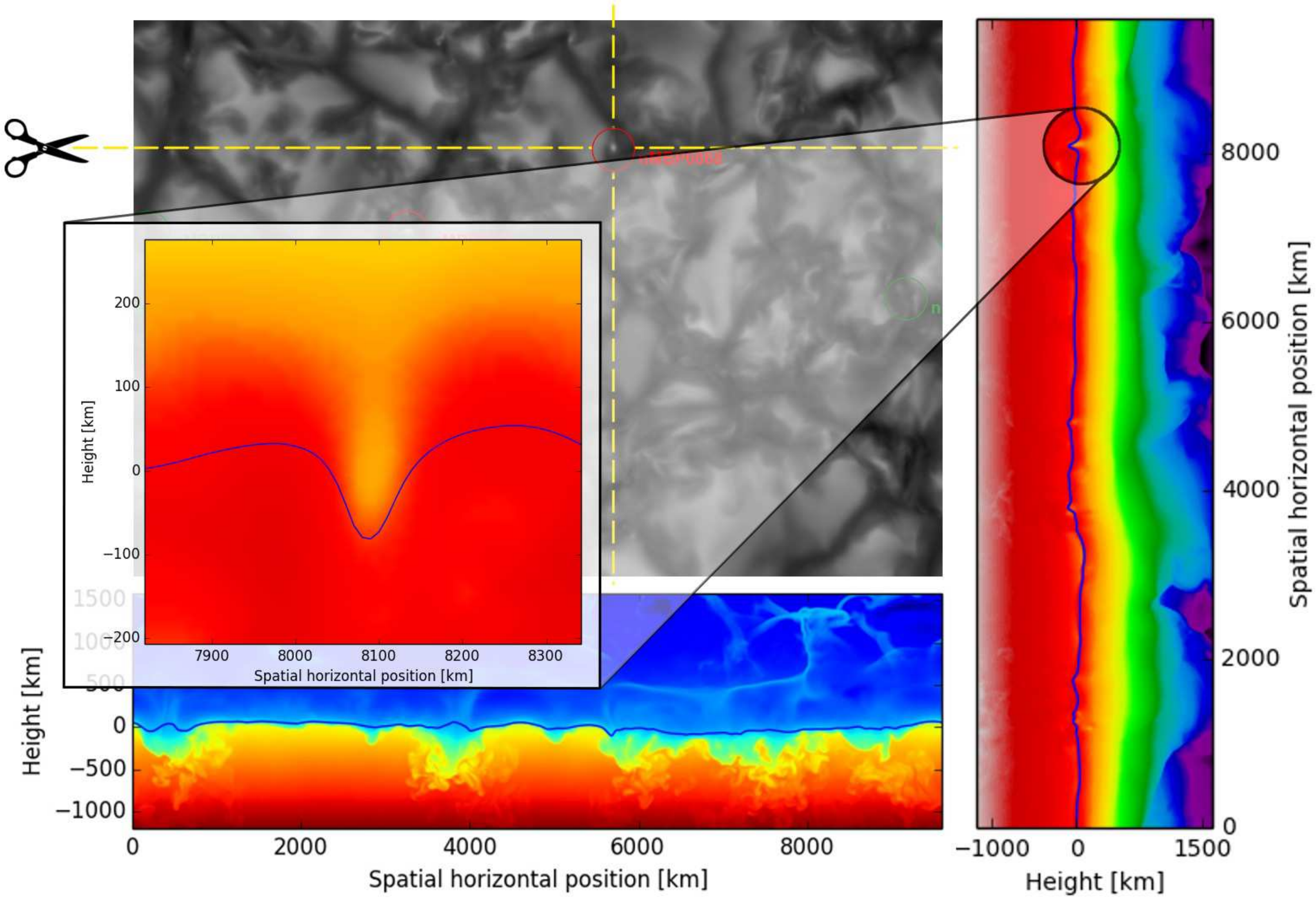

Courtesy, *F. Calvo IRSOL*.

Emergent intensity I (*top left*), temperature T (*bottom*), density $\log(\rho)$ (*right*)

Numerical simulations at IRSOL (cont.)

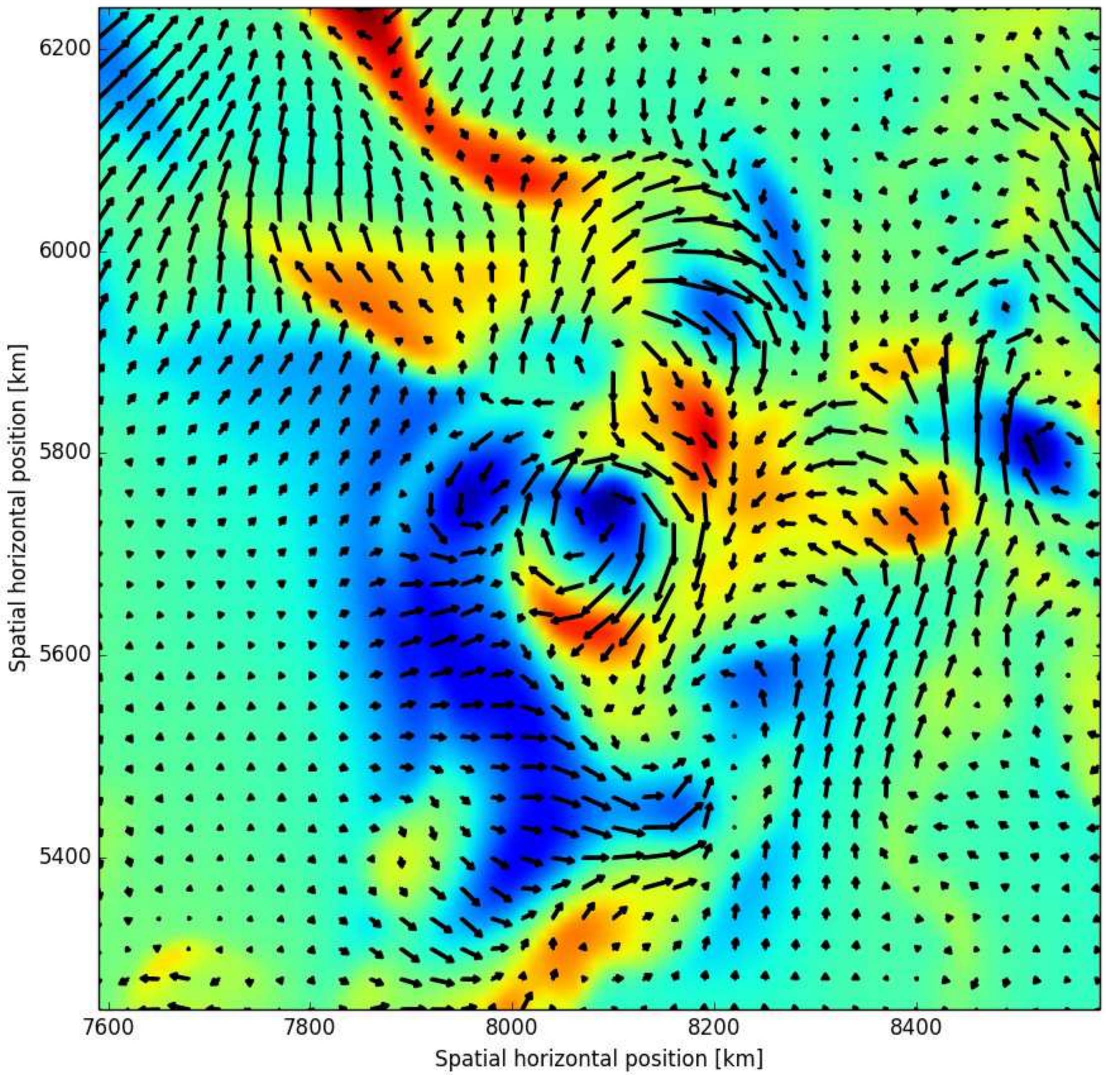

non-magnetic bright points (nMBPs) are locations with:

- *swirling motion* (but ≈ 150 [km] below $\tau = 1$ there are often swirls that do not produce nMBPs);
- *low density* (but a density deficiency alone does not warrant nMBP's);
- *high intensity contrast* (but a local intensity peak does not need to be a nMBP).

Density (blue: low, red: high) and velocity field in an horizontal plane, 150 [km] below $\langle\tau\rangle = 1$

Courtesy, *F. Calvo, IRSOL*.

Numerical simulations at IRSOL (cont.)

Previous investigations of non-magnatic bright points from simulations by *R. Moll et al.* (2011, A&A 533, A126), *B. Freytag* (2013, MSAI 24, 26), *B. Beeck et al.* (2015, A&A 558, A49).

Statistical properties from 256 non-magnetic bright points:

diameter [km] (intensity FWHM)	intensity contrast local [%]	intensity contrast global [%]	mass density contrast [%]	Wilson depression [km]
40 ± 10	20 ± 10	2.3 ± 9	58 ± 10	103 ± 32

Courtesy, *F. Calvo, IRSOL*.

Numerical simulations at IRSOL (cont.)

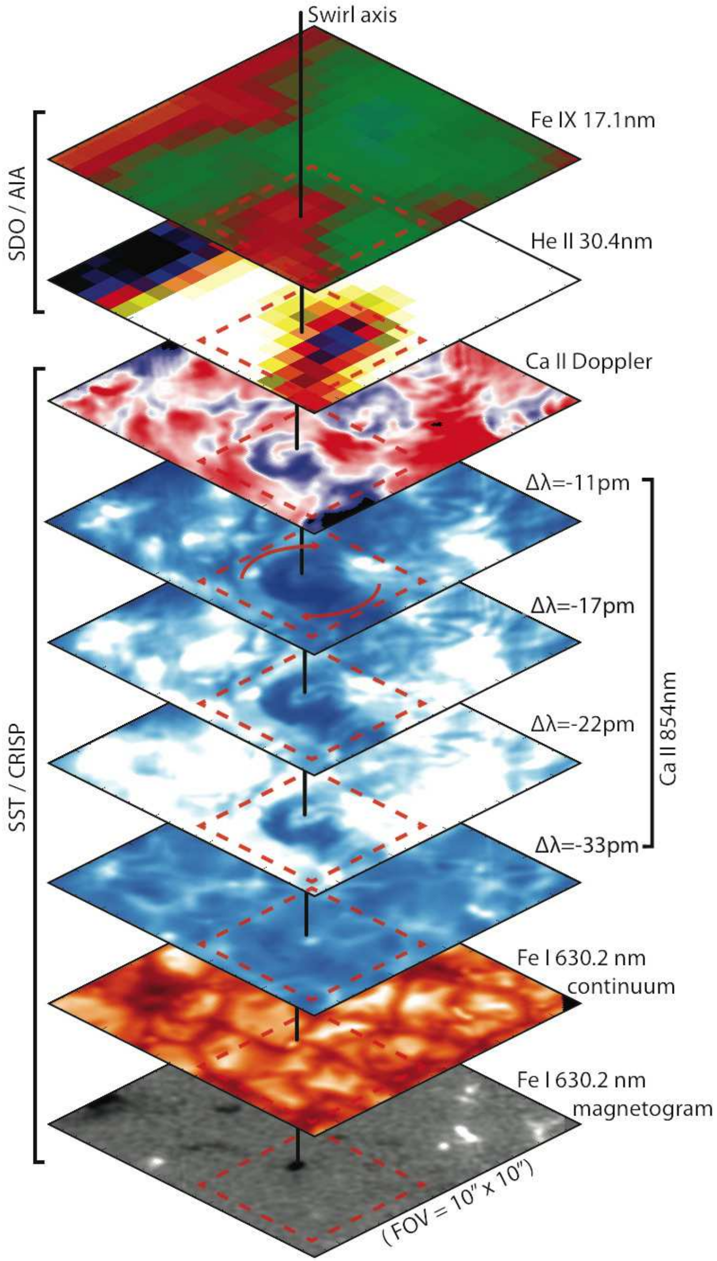

Multi-Waveband Observation:

Layered atmosphere from the *photosphere* (bottom panel: magnetogram, Fe I 630.2 nm continuum), through the *chromosphere* (Dopplergram, Ca II 854.2 nm) and the *transition region* (He II 30.4 nm) to the *low corona* (top: Fe IX 17.1 nm). Co-temporal observations with SDO/AIA (cadence, 12 s; image scale, $0.699''$ per pixel) and SST/CRISP (cadence, 14 s; Ca II 854.2 nm; image scale, $0.0699''$ per pixel). From *Wedemeyer, Scullion, Steiner et al. (2012) Nature 486, 505*.

Numerical simulations at IRSOL (cont.)

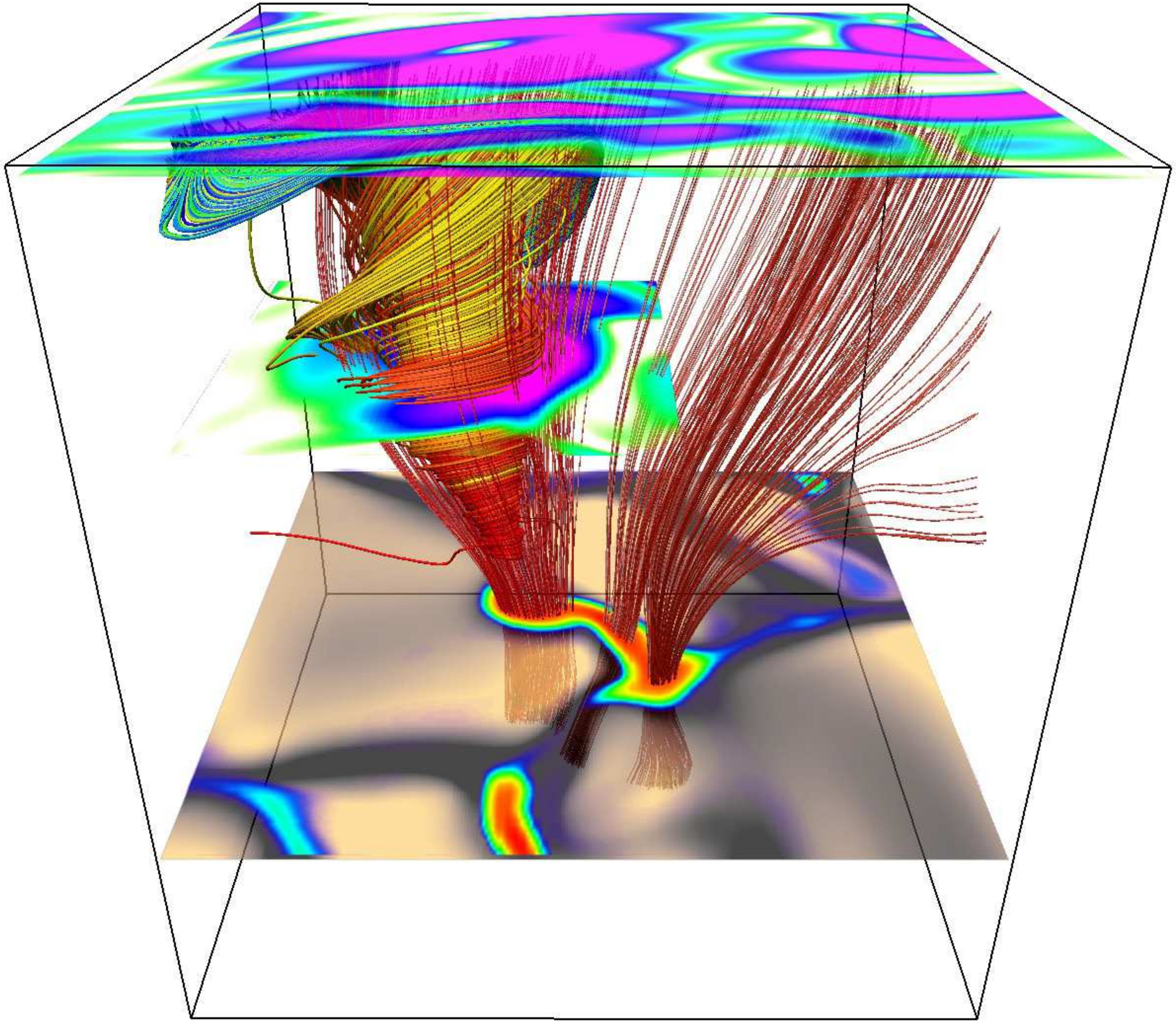

Close-up of a swirl event. The plasma flows along and co-rotates with the magnetic field (spiral streamlines). From *www.solartornado.info*.

3. Polarized radiative transfer in discontinuous media

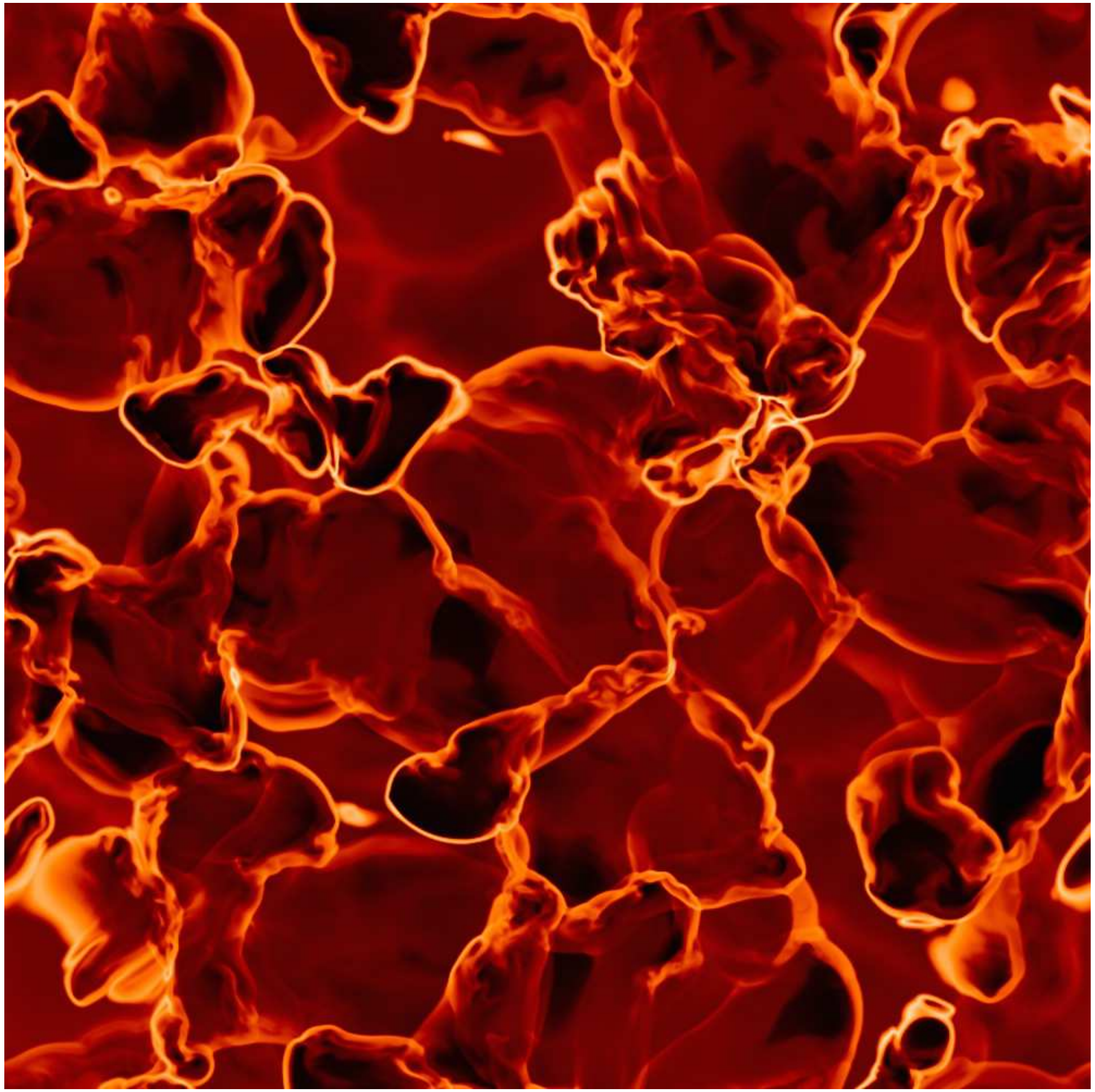

Horizontal cross-section in the chromosphere of a simulation. Colors show temperature. *Shock fronts and temperature spikes* are ubiquitous.

In a *PhD-project at IRSOL*, we test new ideas on numerical methods for polarized radiative transfer in discontinuous media (PhD-project of *Gioele Janett*).

Table of content

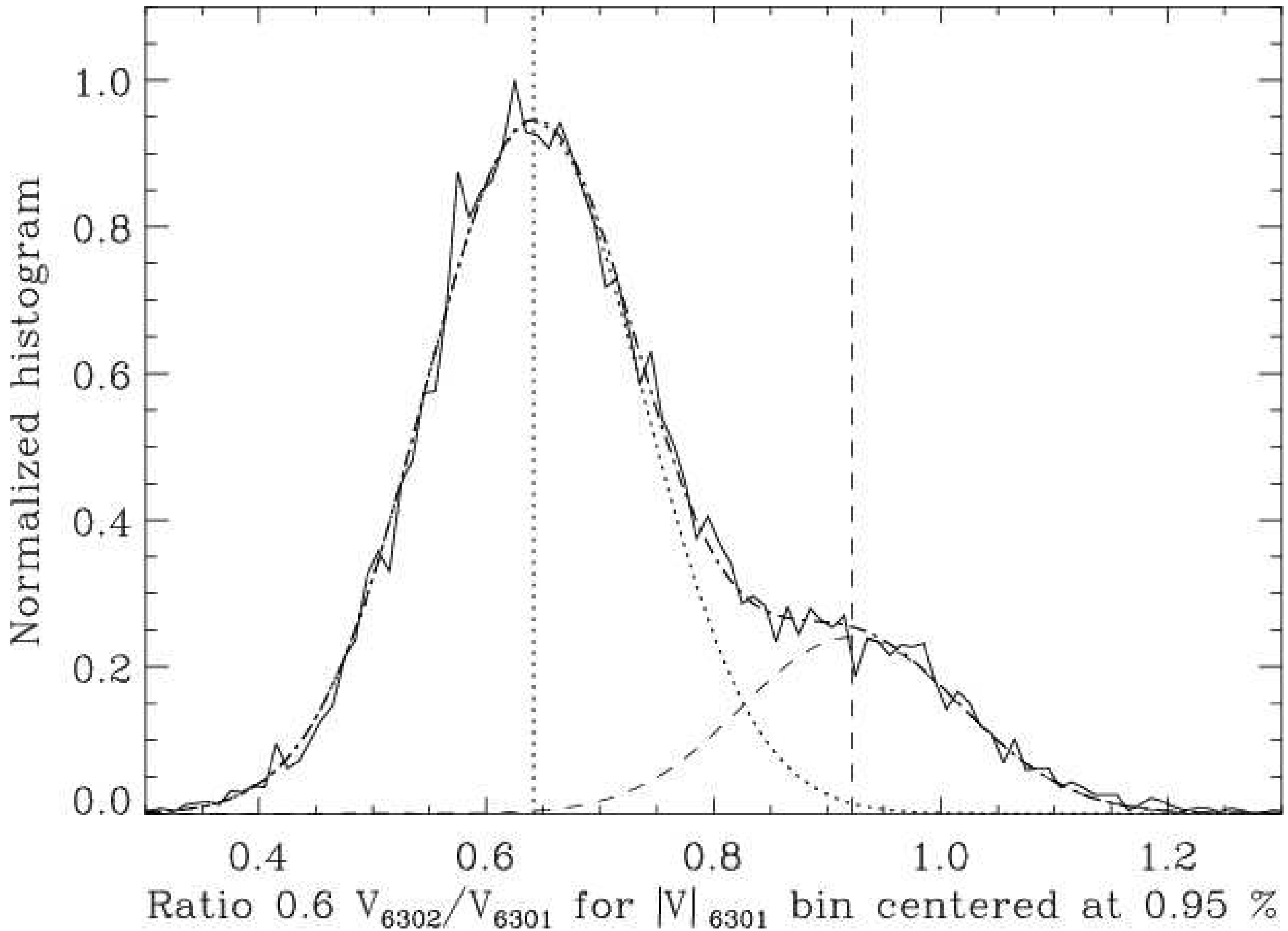

1.0
0.8
0.6
0.4
0.2
0.0
Normalized histogram
0.4
0.6
0.8
1.0
1.2
Ratio 0.6 V6302/V6301 for |V|6301 bin centered at 0.95 %

→ backto § 1.

References

Beeck, B., Cameron, R.H., Reiners, A., & Schüssler, M.: 2013, *Three-dimensional simulations of near-surface convection in main-sequence stars II. Properties of granulation and spectral lines*, A&A 558, A49

Freytag, B.: 2013, *Advances in the hydrodynamics solver of CO5BOLD*, Mem. Soc. Astr. It. Suppl. 24, 26

Moll, R., Cameron, R.H., & Schüssler, M.: 2012, *Vortices in simulations of solar surface convection*, A&A 533, A126

Stenflo, J.O.: 2010, *Distribution functions for magnetic fields on the quiet Sun*, A&A 665, A37

Steiner, O., Rezaei, R.: 2012, *Recent Advances in the Exploration of the Small-Scale Structure of the Quiet Solar Atmosphere: Vortex Flows, the Horizontal Magnetic Field, and the Stokes-V Line-Ratio Method*, in L. Golub, I. De Moortel, and T. Shimizu (eds.), Hinode 5: Exploring the Active Sun, ASP Conf. Ser. 456, p. 3-32.

Steiner, O., Züger, F., & Belluzi, L.: 2015, *Polarized radiative transfer in discontinuous media*, A&A submitted

Wedemeyer-Böhm, S., Scullion, E., Steiner, O., Rouppe van der Voort, L., de la Cruz Rodriguez, J., Fedun, V. & Erdélyi, R.: 2012, *Magnetic tornadoes as energy channels into the solar corona*, Nature **486**, 505-508